Mixed Gold(I)−Gold(III) Complexes with Bridging Selenido Ligands. Theoretical Studies of the Gold(I)−Gold(III) Interactions

Silvia Canales,[†] Olga Crespo,[†] M. Concepción Gimeno,[†] Peter G. Jones,[‡]
Antonio Laguna,*,[†] and Fernando Mendizabal[§]

*Departamento de Química Inorgánica, Instituto de Ciencia de Materiales de Aragón,
Universidad de Zaragoza-CSIC, 50009 Zaragoza, Spain, Institut für Anorganische und
Analytische Chemie der Technischen Universität, Postfach 3329, D-38023 Braunschweig,
Germany, and Facultad de Ciencias, Universidad de Chile, Casilla 653,
Santiago de Chile, Chile*

Received June 4, 2001

The gold(I) compounds [Se(AuPPh₃)₂] and [Se{Au₂(μ-dppf)}] (dppf = 1,1′-bis(diphenylphosphino)ferrocene) react with 1 and 2 equiv of [Au(C₆F₅)₃OEt₂] to give the mixed gold(I)−gold(III) derivatives [Se(AuPPh₃)₂{Au(C₆F₅)₃}ₙ] and [Se{Au₂(μ-dppf)}{Au(C₆F₅)₃}ₙ] (*n* = 1, 2). The reaction of [Se(AuPPh₃)₂] with [Au(C₆F₅)₂Cl]₂ affords the complex [{Se(AuPPh₃)}₂{μ-Au(C₆F₅)₂}₂]. The crystal structures of [Se{Au₂(μ-dppf)}{Au(C₆F₅)₃}] and [{Se(AuPPh₃)}₂{μ-Au(C₆F₅)₂}₂] have been characterized by X-ray diffraction studies. They show dissimilar Au(I)···Au(III) distances, indicating the presence of weak interactions. Quasi-relativistic pseudopotential calculations on [Se(AuPH₃)₂(AuR₃)], [Se(AuPH₃)(AuR₃)₂]⁻ (R = −H, −CH₃), and [{Se(AuPH₃)}₂{Au(CH₃)₂}₂] models have been performed at Hartree−Fock and second-order Møller−Plesset perturbation theory levels. There is a good agreement between experimental and theoretical geometries at the MP2 level.

Introduction

A strongly attractive and energetically favorable interaction has been observed between gold(I) atoms with d¹⁰ configurations in numerous polynuclear gold compounds. The attraction between closed-shell systems of the type d¹⁰−d¹⁰ and d¹⁰−d⁸ among heavy metals has been classified as a metallophilic or van der Waals type.[1] Experimental evidence for the aurophilic Au(I)···Au(I) attraction is available from crystallography, NMR and Raman spectroscopy, and optical spectroscopic measurements of the interaction strength.[2] It is manifested in molecular conformations with metal−metal distances generally of ca. 3.0 Å and surprisingly high bond

energies, 5−15 kcal/mol, similar to or even higher than for conventional hydrogen bonding.[2] This type of interaction has been the subject of a number of theoretical treatments. The dispersion forces, essential in the stabilization of the systems that show these interactions, are not found at the HF (Hartree−Fock) level. Therefore, it is necessary to use at least MP2 (second-order Møller−Plesset perturbation theory)[3] level methods for the complete description of the dispersion forces, which are included among the correlation effects.[4]

We are currently working on chalcogenide-centered gold complexes, and we have previously reported the synthesis of several sulfur-centered complexes of gold-(I) and gold(III);[5] also, we have described the preparation of selenium-centered gold(I) species,[6] together with the theoretical studies of the found structures. In both cases we have described the first example of a quadruply

---

[†] Universidad de Zaragoza-CSIC.
[‡] Institut für Anorganische und Analytische Chemie der Technischen Universität.
[§] Universidad de Chile.

(1) (a) Schmidbaur, H. *Chem. Soc. Rev.* **1995**, 391. (b) Laguna, A. In *Gold, Progress in Chemistry, Biochemistry and Technology*; Schmidbaur, H., Ed.; Wiley: New York, 1999. (c) Schmidbaur, H. *Pure Appl. Chem.* **1993**, *65*, 691. (d) Gimeno, M. C.; Laguna, A. *Gold Bull.* **1999**, *32*, 90. (e) Crespo, O.; Gimeno, M. C.; Laguna, A. *Metal Clusters in Chemistry*; Braunstein, P., Oro, L. A., Raithby, P. R., Eds.; Wiley-VCH: Weinheim, Germany, 1999. (f) Crespo, O.; Laguna, A.; Fernández, E.; López-de-Luzuriaga, J.; Jones, P.; Teichert, M.; Monge, M.; Pyykkö, P.; Runeberg, N.; Schütz, M.; Werner, H. *Inorg. Chem.* **2000**, *39*, 4786.

(2) (a) Jones, P. G. *Gold Bull.* **1981**, *14*, 102. (b) Schmidbaur, H. *Gold Bull.* **1990**, *23*, 11. (c) Gade, L. H. *Angew. Chem., Int. Ed. Engl.* **1997**, *36*, 1171. (d) Mansour, M. A.; Connick, W. B.; Lachicotte, R. J.; Gysling, H. J.; Eisenberg, R. J. *J. Am. Chem. Soc.* **1998**, *120*, 1329. (e) Dziwok, K.; Lachmann, J.; Wilkinson, D. L.; Müller, G.; Schmidbaur, H. *Chem. Ber.* **1990**, *123*, 423. (f) Schmidbaur, H.; Graf, W.; Müller, G. *Angew. Chem., Int. Ed. Engl.* **1988**, *27*, 417. (g) Narayanaswamy, R.; Young, M. A.; Parkhurst, E.; Ouellette, M.; Kerr, M. E.; Ho, D. M.; Elder, R. C.; Bruce, A. E.; Bruce, M. R. M. *Inorg. Chem.* **1993**, *32*, 2506. (h) Harwell, M. E.; Mortimer, M. D.; Knobler, C. B.; Anet, F. A. L.; Hawthorne, M. F. *J. Am. Chem. Soc.* **1996**, *118*, 2679.

(3) Møller, C.; Plesset, M. S. *J. Chem. Phys.* **1934**, *46*, 618.

(4) (a) Pyykkö, P. *Chem. Rev.* **1997**, *97*, 597. (b) Pyykkö, P.; Zhao, Y.-F. *Angew. Chem.* **1991**, *103*, 622. (c) Pyykkö, P.; Li, L.; Runeberg, N. *Chem. Phys. Lett.* **1994**, *218*, 133. (d) Pyykkö, P.; Mendizabal, F. *Inorg. Chem.* **1998**, *37*, 3018. (e) Runenberg, N.; Schütz, M.; Werner, H.-J. *J. Chem. Phys.* **1999**, *110*, 7210.

(5) (a) Canales, F.; Gimeno, M. C.; Jones, P. G.; Laguna, A. *Angew. Chem., Int. Ed. Engl.* **1994**, *33*, 769. (b) Canales, F.; Gimeno, M. C.; Laguna, A.; Villacampa, M. D. *Inorg. Chim. Acta* **1996**, *244*, 95. (c) Canales, F.; Gimeno, M. C.; Jones, P. G.; Laguna, A. *J. Am. Chem. Soc.* **1996**, *118*, 4839. (d) Canales, F.; Gimeno, M. C.; Laguna, A.; Jones, P. G. *Organometallics* **1996**, *15*, 3412. (e) Calhorda, M. J.; Canales, F.; Gimeno, M. C.; Jiménez, J.; Jones, P. G.; Laguna, A.; Veiros, L. F. *Organometallics* **1997**, *16*, 3837. (f) Canales, F.; Canales, S.; Crespo, O.; Gimeno, M. C.; Jones, P. G.; Laguna, A. *Organometallics* **1998**, *17*, 1617.

(6) (a) Canales, S.; Crespo, O.; Gimeno, M. C.; Jones, P. G.; Laguna, A. *J. Chem. Soc., Chem. Commun.* **1999**, 679. (b) Canales, S.; Crespo, O.; Gimeno, M. C.; Jones, P. G.; Laguna, A.; Mendizabal, F. *Organometallics* **2000**, *19*, 4985.

Scheme 1[a]
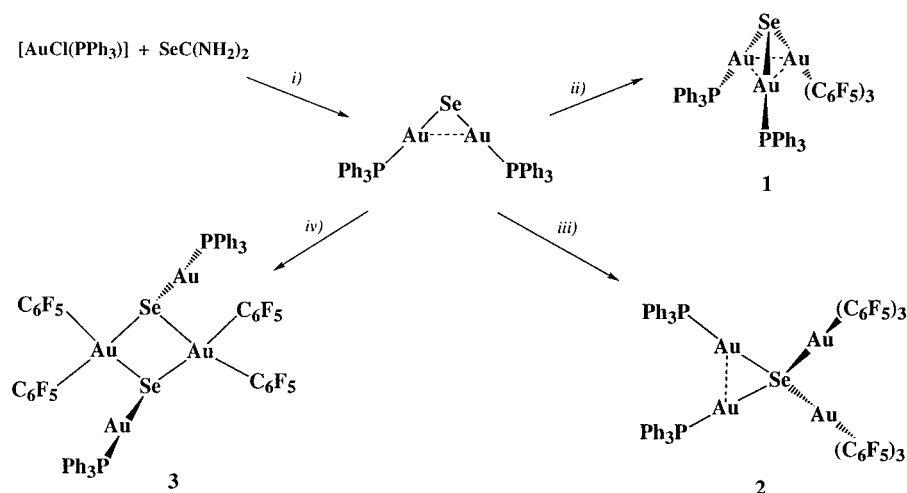
[a] Legend: (i) $MeOH$, Na_2CO_3; (ii) $[Au(C_6F_5)_3OEt_2]$; (iii) 2 $[Au(C_6F_5)_3OEt_2]$; (iv) $[Au(C_6F_5)_2Cl]_2$.

bridging sulfido or selenido ligand. Here we report the synthesis of mixed-valence selenium-centered derivatives whose crystal structures have revealed the presence of gold(I)−gold(I) and gold(I)−gold(III) interactions. Our aim is to determine the length and estimate the strength of these contacts, which are present between gold(I) and gold(III) in the complexes described here, and to compare them with corresponding parameters of gold(I)−gold(I) interactions. For this we will use quasi-relativistic pseudopotential calculations at the Hartree−Fock and second-order Møller−Plesset perturbation theory levels.

Results and Discussion

The reaction of the gold(I) complex $[Se(AuPPh_3)_2]$ with 1 and 2 equiv of $[Au(C_6F_5)_3OEt_2]$ gives the mixed gold-(I)−gold(III) derivatives $[Se(AuPPh_3)_2\{Au(C_6F_5)_3\}]$ (**1**) and $[Se(AuPPh_3)_2\{Au(C_6F_5)_3\}_2]$ (**2**), respectively. The products are air-stable colorless solids that behave as nonconductors in acetone solutions. The IR spectra show absorptions at around 1505 (s), 996 (s), 805 (s), and 795 (s) cm^{-1} arising from the presence of pentafluorophenyl groups bonded to a gold(III) center.

The $^{31}P\{^1H\}$ NMR spectra show a sharp singlet resonance at 35.4 (**1**) and 35.6 ppm (**2**), indicating the equivalence of both phosphorus groups. The low-temperature NMR spectra show a different behavior because the spectrum of compound **1** splits into two resonances, whereas the single resonance of complex **2** remains unchanged. This is probably attributable to the presence of a weak gold(I)−gold(III) interaction in compound **1**, which renders the phosphorus atoms inequivalent. In complex **2** this type of interaction is absent, probably because the tetrahedral geometry around the selenium atom does not allow short gold-(I)−gold(III) interactions.

The ^{19}F NMR spectra show a typical pattern for a tris-(pentafluorophenyl) derivative, consisting of six signals in a 2:1 ratio for the trans and cis pentafluorophenyl groups. Each group presents two multiplets for the ortho and meta fluorine and a triplet for the para fluorine. At low temperature the rotation of the pentafluorophenyl rings is restricted, and then the spectrum of **1** shows

four multiplets for the ortho and meta fluorine in the ratio 2:2:1:1 and two triplets for the para fluorine in a ratio 2:1.

In the positive liquid secondary-ion mass spectra (LSIMS+) the molecular peaks do not appear but the fragments arising at the loss of pentafluorophenyl units are present at m/z 1529 (11%) $[Se(AuPPh_3)_2Au(C_6F_5)_2]^+$ and 1195 (14%) $[Se(AuPPh_3)_2Au]^+$.

The structure of these compounds has not been established without ambiguity, but we propose (see Scheme 1) for complex **1** a structure similar to that reported below with 1,1′-bis(diphenylphosphino)ferrocene (dppf) as the ligand, consisting of a trigonal pyramid with basal gold atoms and selenium at the apex. The structure of complex **2** may be similar to that found in the related sulfur species, $[S(AuPPh_3)_2\{Au-(C_6F_5)_3\}_2]$, previously described by us, which involves a tetrahedral geometry with no short gold−gold interactions.[5c]

The treatment of $[Se(AuPPh_3)_2]$ with the gold(III) compound $[Au(C_6F_5)_2Cl]_2$ in the molar ratio 2:1 leads to the mixed species $[\{Se(AuPPh_3)\}_2\{\mu\text{-}Au(C_6F_5)_2\}_2]$ (**3**), with $[AuClPPh_3]$ as byproduct. The mixture could not be separated, and thus in the spectroscopic data both compounds were observed and the analytical data are not reliable.

In the $^{31}P\{^1H\}$ NMR spectrum the resonance for $[AuClPPh_3]$ is easily identifiable and one more resonance appears for compound **3** as a consequence of the equivalence of the phosphorus atoms. The low-temperature NMR spectrum also shows only one signal for the two phosphorus atoms. The ^{19}F NMR spectrum presents three signals for the equivalent pentafluorophenyl units. At −55 °C these three signals split into five due to the lack of rotation of the pentafluorophenyl rings.

In the LSIMS+ spectrum the molecular peak appears at m/z 2138 (1%); fragmentation peaks are produced for the loss of $AuPPh_3^+$ at m/z 1681 (7%).

The crystal structure of complex **3** has been established by an X-ray diffraction study, and the molecule is shown in Figure 1. A selection of bond lengths and angles is collected in Table 1. The molecule displays crystallographic inversion symmetry. It consists of two "$SeAu(PPh_3)$" units bridged by two "$Au(C_6F_5)_2$" frag-
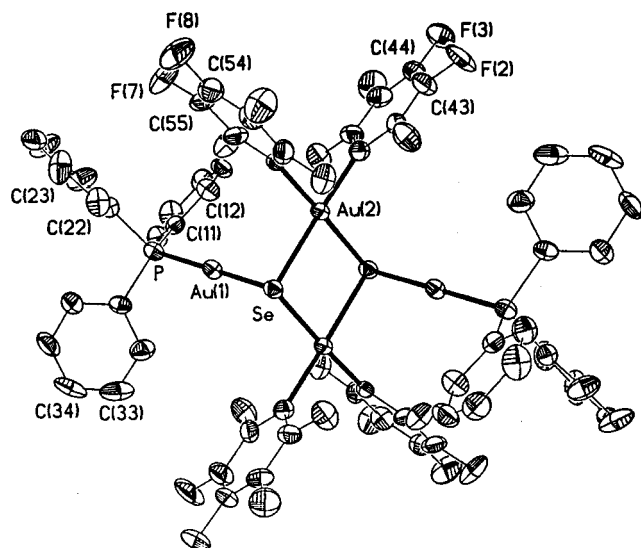
Figure 1. Structure of complex **3** in the crystal form with the atom-numbering scheme. Displacement parameter ellipsoids represent 50% probability surfaces. The H atoms are omitted for clarity.

Table 1. Selected Bond Lengths (Å) and Angles (deg) for Complex 3[a]

Au(1)−P	2.273(2)	Au(2)−C(51)	2.070(7)
Au(1)−Se	2.4225(9)	Au(2)−Se	2.4802(8)
Au(2)−C(41)	2.046(8)		
P−Au(1)−Se	175.14(5)	Au(2)−Se−Au(2)#1	94.23(3)
C(41)−Au(2)−C(51)	89.7(2)	C(31)−P−Au(1)	110.5(2)
C(41)−Au(2)−Se	177.92(18)	C(21)−P−Au(1)	111.3(2)
C(51)−Au(2)−Se	92.37(17)	C(11)−P−Au(1)	116.3(2)
C(41)−Au(2)−Se#1	92.14(18)	C(42)−C(41)−Au(2)	122.2(5)
C(51)−Au(2)−Se#1	177.94(18)	C(46)−C(41)−Au(2)	121.9(5)
Se−Au(2)−Se#1	85.77(3)	C(52)−C(51)−Au(2)	123.4(5)
Au(1)−Se−Au(2)	88.20(3)	C(56)−C(51)−Au(2)	119.6(5)
Au(1)−Se−Au(2)#1	95.82(3)		

[a] Symmetry transformations used to generate equivalent atoms: (#1) $-x$, $-y$, $-z + 1$.

ments. Because of the symmetry the Se, Au(2), Se#1 and Au(2)#1 atoms exhibit a perfect rhomboidal arrangement, with internal angles of 85.77(3)° at gold and 94.23(3)° at selenium. Association of two "SeAu$_3$" cores has been described in [Se(AuPPh$_3$)$_3$]$^{+ 7}$ and [(Au$_2$dppf)-{Se(Au$_2$dppf)}$_2$](OTf)$_2$.[6b] In the first case the association is only supported by gold···gold interactions, whereas in the second, there are further interactions with an "Au$_2$dppf" unit connecting two "Se(Au$_2$dppf)" fragments. The compound [Au{Se(Au$_2$dppf)}$_2$]NO$_3$[6b] also contains triply bridging selenide ligands, but the geometry is more complicated; two "Au{Se(Au$_2$dppf)}$_2$" units are bonded through gold···gold interactions over and above those responsible for the association of "SeAu$_3$" cores. Compound **3** exhibits two triply bridging selenide ligands. The structure is not supported by gold···gold interactions; the geometry is more comparable to that in [{S(Au$_2$dppf)}$_2${Au(C$_6$F$_5$)$_2$}]OTf,[5] in which two "S(Au$_2$dppf)" units are bridged by an "Au(C$_6$F$_5$)$_2$" fragment. The shorter gold(I)−gold(III) distance, Au(1)−Au(2) = 3.4120-(6) Å, lies between those found in [{S(Au$_2$dppf)}$_2${Au-(C$_6$F$_5$)$_2$}]OTf (3.2195(8), 3.366(1), 3.799(1) Å; the shortest of these distances are comparable to those of Au(I)−

Au(I) interactions). As expected, the narrowest Au−Se−Au angle, Au(1)−Se−Au(2) = 88.20(3)°, corresponds to the shorter Au−Au distance, the other angle Au(1)−Se−Au(2)#1 is 95.82(3)° with an Au(1)−Au(2)#1 distance of 3.6385(6) Å. The gold center lies in the plane formed by the Se, Se#1, C(41), and C(51) atoms and exhibits square-planar geometry; the narrowest angle is that in the four-membered ring. The Au^{III}−Se distances, Au(2)−Se = 2.4802(8) Å, are similar to that found in [AuCl$_3$(SePh$_2$)] (2.445(1) Å).[8] The Au−C distances are somewhat dissimilar (Au−C(41) = 2.046(8) Å, Au−C(51) = 2.070(7) Å), with the shortest trans to the selenide ligand of the same asymmetrical unit. The linear geometry exhibited by the Au(1) center is slightly distorted (P−Au(1)−Se = 175.14(5)°). The Au^I−Se distance (Au(1)−Se = 2.4225(9) Å) is similar to the shortest distance found in [(Au$_2$dppf){Se(Au$_2$dppf)}$_2$]-(OTf)$_2$ (2.4240(10)−2.4704(10) Å). The value of 2.273-(2) Å found for the Au(1)−P distance is of the same order as the highest value found in [(Au$_2$dppf){Se(Au$_2$dppf)}$_2$]-(OTf)$_2$ (2.259(3)−2.280(2) Å). Both distances compare well with those found in [Se(AuPPh$_3$)$_3$]PF$_6$.[7]

The reaction of [Se{Au$_2$(μ-dppf)}] with 1 and 2 equiv of [Au(C$_6$F$_5$)$_3$OEt$_2$] affords the mixed-valence compounds [Se{Au$_2$(μ-dppf)}{Au(C$_6$F$_5$)$_3$}] (**4**) and [Se{Au$_2$(μ-dppf)}-{Au(C$_6$F$_5$)$_3$}$_2$] (**5**), respectively (Scheme 2). Complexes **4** and **5** are air- and moisture-stable orange solids that are nonconductors in acetone solutions. Their IR spectra show the absorptions arising from the pentafluorophenyl groups bonded to a gold(III) center. The ^{31}P{^{1}H} NMR spectra present one singlet for the equivalent phosphorus atoms. The ^{1}H NMR spectra show, apart from the multiplets due to the phenylic protons, two broad multiplets for the α- and β-protons of the cyclopentadienyl rings. The low-temperature NMR spectrum is different for complex **4** or **5**; for compound **4** in the ^{1}H NMR spectrum the cyclopentadienyl protons are inequivalent and then seven resonances appear in the ratio 1:1:2:1:1:1:1 for the eight protons, whereas the ^{31}P{^{1}H} NMR spectrum shows two signals for the two different phosphorus atoms. Again the different gold-(I)−gold(III) distances may be responsible for the inequivalence of the two phosphorus atoms. For compound **5** the ^{1}H NMR spectrum at low temperature shows four resonances for the cyclopentadienyl protons, whereas the ^{31}P{^{1}H} NMR spectrum shows the same pattern as at room temperature.

In the LSIMS+ spectrum of **4** the molecular peak does not appear but the fragment arising at the loss of one pentafluorophenyl unit appears at m/z 1558 (41%). For compound **5** the molecular peak is also not present, but the fragment at m/z 2254 (7%), arising at the loss of two pentafluorophenyl units, is observed.

The structure of complex **4** has been determined by X-ray diffraction studies, and the molecule is shown in Figure 2. Selected bond lengths and angles are collected in Table 2. The selenido ligand is bonded to two gold(I) atoms of an "Au$_2$(μ-dppf)" unit, with a gold−gold contact of 2.9457(9) Å, and to a gold(III) center. The structure of the heavy-atom core is therefore trigonal pyramidal with the selenium at the apex, lying 1.408 Å out of the plane formed by the three gold atoms. The structure is similar to those obtained for the trinuclear gold(I)

(7) Lensch, C.; Jones, P. G.; Sheldrick; G. M. Z. *Naturforsch., B* **1982**, *37B*, 944.

(8) Jones, P. G.; Thöne, C. *Z. Naturforsch., B* **1990**, *46B*, 50.

Scheme 2^a

$$[Au_2Cl_2(\mu\text{-dppf})] + SeC(NH_2)_2$$
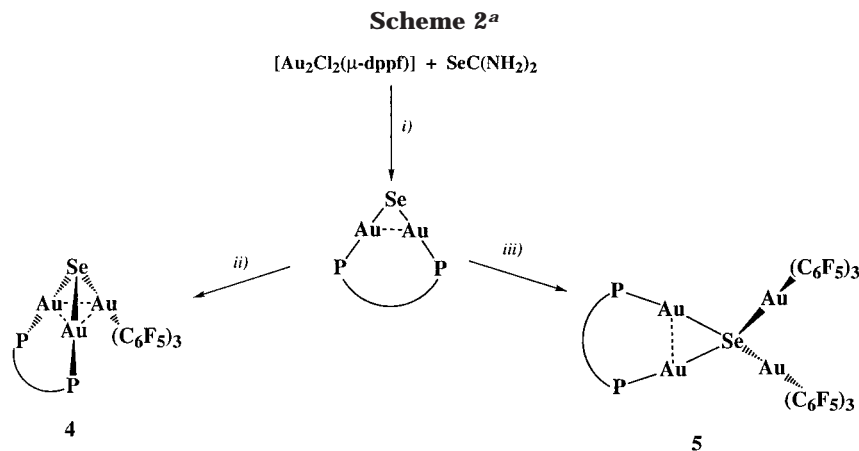
^{a} Legend: (i) MeOH, Na$_2$CO$_3$; (ii) [Au(C$_6$F$_5$)$_3$OEt$_2$]; (iii) 2 [Au(C$_6$F$_5$)$_3$OEt$_2$].
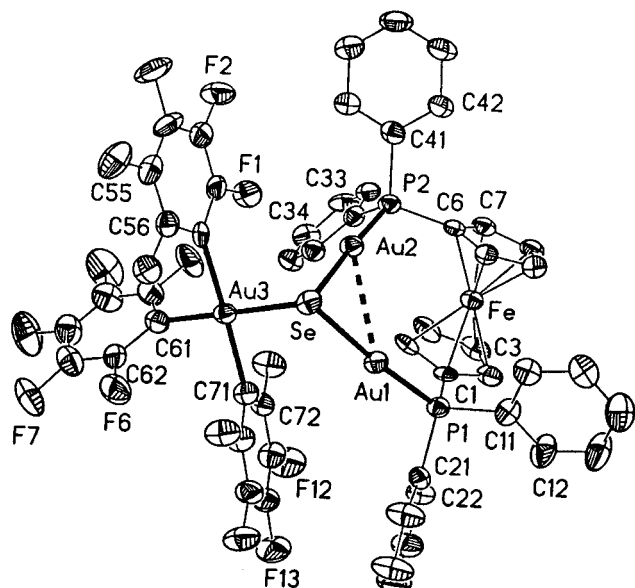

Figure 2. Structure of complex **4**. Displacement parameter ellipsoids represent 50% probability surfaces. The H atoms are omitted for clarity.

Table 2. Selected Bond Lengths (Å) and Angles (deg) for Complex 4

Au(1)−P(1)	2.266(3)	Au(3)−C(61)	2.060(12)
Au(1)−Se	2.4569(11)	Au(3)−C(71)	2.079(11)
Au(1)−Au(2)	2.9457(9)	Au(3)−C(51)	2.079(11)
Au(2)−P(2)	2.269(3)	Au(3)−Se	2.5038(13)
Au(2)−Se	2.4486(12)		
P(1)−Au(1)−Se	174.16(7)	Au(1)−Se−Au(3)	103.63(4)
P(1)−Au(1)−Au(2)	121.34(7)	C(1)−P(1)−Au(1)	111.0(3)
Se−Au(1)−Au(2)	52.97(3)	C(11)−P(1)−Au(1)	115.8(3)
P(2)−Au(2)−Se	175.51(8)	C(21)−P(1)−Au(1)	113.9(3)
P(2)−Au(2)−Au(1)	122.77(7)	C(6)−P(2)−Au(2)	109.7(3)
Se−Au(2)−Au(1)	53.23(3)	C(31)−P(2)−Au(2)	112.3(3)
C(61)−Au(3)−C(71)	88.8(4)	C(41)−P(2)−Au(2)	115.4(3)
C(61)−Au(3)−C(51)	90.2(4)	C(56)−C(51)−Au(3)	121.7(7)
C(71)−Au(3)−C(51)	177.5(3)	C(52)−C(51)−Au(3)	124.3(7)
C(61)−Au(3)−Se	177.7(2)	C(66)−C(61)−Au(3)	123.4(7)
C(71)−Au(3)−Se	92.4(3)	C(62)−C(61)−Au(3)	121.7(8)
C(51)−Au(3)−Se	88.4(3)	C(76)−C(71)−Au(3)	121.0(7)
Au(2)−Se−Au(1)	73.81(3)	C(72)−C(71)−Au(3)	122.7(7)
Au(2)−Se−Au(3)	91.01(4)		

derivatives with a central selenium atom[6b,7] that present short gold−gold contacts. In this molecule the shortest distance corresponds to gold(I)−gold(I), 2.9457(9) Å, which is of the same order as that found in the starting material, [Se{Au$_2$(μ-dppf)}],[6b] and there are two dis-

similar Au(I)−Au(III) distances, 3.5330(8) and 3.8993-(8) Å, one much shorter than the other. These distances are of the same order as those obtained for the similar complex with a bridging sulfido ligand, 3.404(1) and 3.759(1) Å.[5d] These data indicate the existence of an Au-(I)⋯Au(III) interaction that, although weak, is able to reduce the symmetry in the molecule and thus render the gold(I) atoms inequivalent, as also detected in the ^{31}P{^{1}H} NMR spectrum. The Au−Se−Au angles are also dissimilar. Of necessity, narrower Au−Se−Au angles are correlated with shorter gold−gold contacts, and thus the narrower angle corresponds to that between the two gold(I) atoms, Au(1)−Se−Au(2) = 73.81(3)°, whereas the angles subtended by the gold(I) and the gold(III) atoms are 91.01(4) and 103.63(4)°. The Au−Se distances to the gold(I) atoms are 2.4486(12) and 2.4569(11) Å, slightly longer than those in the starting material, 2.4218(11) and 2.4055(11) Å.[6b] The Au^{III}−Se bond distance of 2.5038(13) Å is longer than that found in complex **3** and also in [AuCl$_3$(SePh$_2$)] (2.445(1) Å).[8] The geometry for the gold atoms is in accordance with their oxidation state, with a slight deviation of the gold(I) atoms from linearity (angles 174.16(7) and 175.51(8)°).

Theoretical Calculations. The compounds described in the Experimental Section show Au^I−Au^I, Au^I−Au^{III}, and Au^{III}−Au^{III} contacts. It is observed that as the oxidation state of the gold center increases the metal−metal distance increases, and thus the order is Au^{III}−Au^{III} > Au^{III}−Au^I > Au^I−Au^I. We have carried out ab initio calculations at the MP2 and HF levels with quasi-relativistic pseudopotentials with the objective of understanding the origin of metal−metal interactions.

In complex **4**, [Se{Au$_2$(μ-dppf)}{Au(C$_6$F$_5$)$_3$}], the two Au(I) centers are separated by 2.95 Å and are bridged by a ferrocenyl phosphine. This distance is classical in gold(I) complexes. The two Au^I−Au^{III} distances, on the other hand, are 3.53 and 3.89 Å, whose average is 3.72 Å. These data indicate the existence of a weak but important Au^I−Au^{III} interaction. Similar short distances involving gold(III) are observed in the compound **3**, [{Se-(AuPPh$_3$)}$_2${μ-Au(C$_6$F$_5$)$_2$}$_2$]; that between Au(I) and Au-(III) is 3.41 Å and that between Au(III) and Au(III) is 3.63 Å, clearly longer than those observed for Au^I−Au^I systems.

In addition to the models [Se(AuPH$_3$)$_2$(AuR$_3$)] (R = −H (a), −CH$_3$ (b)) and [(Se(AuPH$_3$))$_2$(Au(CH$_3$)$_2$)$_2$] (e), which represent the experimental complexes, we have

Table 3. Main Parameters of the Selenium-Centered Systems (Distances in Å)

system	method	Se−Au^I	Se−Au^{III}	Au^I−Au^I	Au^I−Au^{III}	Au^{III}−Au^{III}
[Se(Au$_2$dppf){Au(C$_6$F$_5$)$_3$}]	exptl	2.453	2.504	2.946	3.72 (3.53/3.89)	
[{Se(AuPPh$_3$)}$_2${Au(C$_6$F$_5$)$_2$}$_2$]	exptl	2.423	2.480		3.412	3.634
[Se(AuPH$_3$)$_2$(AuH$_3$)] (C_s) (a)	HF	2.483	2.661	3.648	3.729	
	MP2	2.452	2.664	2.937	3.545	
[Se(AuPH$_3$)$_2${Au(CH$_3$)$_3$}] (C_s) (b)	HF	2.481	2.584	3.640	3.717	
	MP2	2.453	2.551	2.930	3.602	
[Se(AuPH$_3$)(AuH$_3$)$_2$]$^-$ (C_s) (c)	HF	2.471	2.636		3.562	4.266
	MP2	2.423	2.552		3.346	3.494
[Se(AuPH$_3$){Au(CH$_3$)$_3$}$_2$]$^-$ (C_s) (d)	HF	2.473	2.582		3.862	4.310
	MP2	2.432	2.547		3.615	3.970
[{Se(AuPH$_3$)}$_2${Au(CH$_3$)$_2$}$_2$](C_s) (e)	HF	2.458	2.623		3.895	3.899
	MP2	2.431	2.551		3.477	3.702

Table 4. Main Parameters of the Selenium-Centered Systems (Distances in Å and Angles in deg)

system	method	Au−H	Au−C	Au−P	Au^I−Se−Au^I	Au^I−Se−Au^{III}	Au^{III}−Se−Au^{III}
[Se(Au$_2$dppf){Au(C$_6$F$_5$)$_3$}]	exptl		2.062	2.255	73.8	91.0	
[{Se(AuPPh$_3$)}$_2${Au(C$_6$F$_5$)$_2$}$_2$]	exptl		2.070	2.273		88.2	94.2
[Se(AuPH$_3$)$_2$(AuH$_3$)] (C_s) (a)	HF	1.617		2.410	94.55	92.8	
	MP2	1.627		2.307	73.58	80.0	
[Se(AuPH$_3$)$_2${Au(CH$_3$)$_3$}] (C_s) (b)	HF		2.083	2.412	94.20	94.4	
	MP2		2.068	2.313	73.61	92.1	
[Se(AuPH$_3$)(AuH$_3$)$_2$]$^-$ (C_s) (c)	HF	1.623		2.393		88.39	108.1
	MP2	1.633		2.279		84.52	86.4
[Se(AuPH$_3$){Au(CH$_3$)$_3$}$_2$]$^-$ (C_s) (d)	HF		2.082	2.384		99.6	113.3
	MP2		2.066	2.285		93.1	102.4
[{Se(AuPH$_3$)}$_2${Au(CH$_3$)$_2$}$_2$](C_s) (e)	HF		2.079	2.407		100.1	96.04
	MP2		2.071	2.407		87.9	93.1
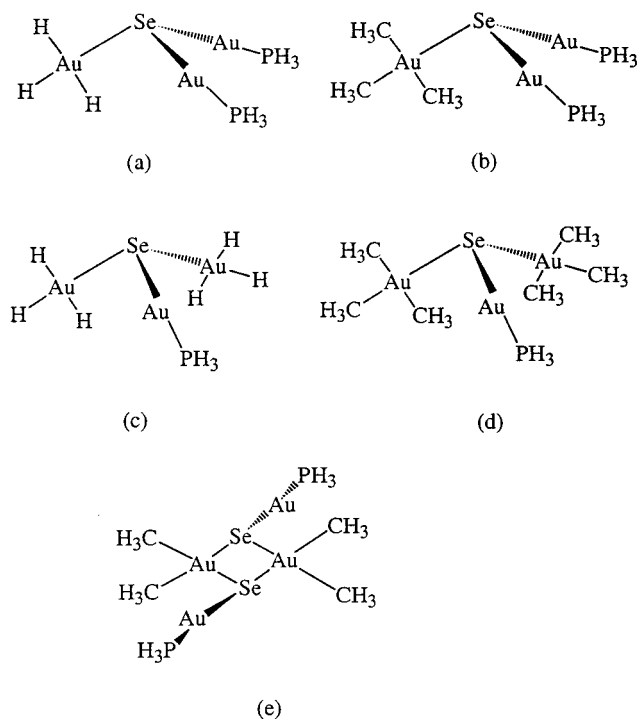
Figure 3. Geometries of the models.

included one hypothetical cluster: [Se(AuPH$_3$)(AuR$_3$)$_2$]$^-$ (R = −H (c), −CH$_3$ (d)). This will complete the range of the Au^I−Au^{III} and Au^{III}−Au^{III} interactions in the systems under study.

The optimized geometries are shown in Tables 3 and 4, together with relevent experimental structural data. The models are illustrated in Figure 3. It can be seen that the structural parameters change substantially when they are compared at HF and MP2 levels. The gold−gold distances and Au−Se−Au angles are significantly shortened for the latter method and comparable in magnitude to the experimental values. This allows an estimation of the contribution of the electronic correlation to the intramolecular contacts for these clusters. Since it has been suggested that aurophilic attraction is primarily a correlation effect, when we compare the results at HF level, we can recognize the real effect of the electronic correlation.[4]

[Se(AuPH$_3$)$_2$(AuR$_3$)]. This model was partially optimized with C_s symmetry, although the real cluster does not exhibit this symmetry, as one Au^I−Au^{III} distance is shorter than the other. The distance Au-(III)-R (R = −H and −CH$_3$) is also allowed to change, but not the square-planar Au(III) environment. The final geometry around the selenium atom is pyramidal, with shorter Se−Au(I) than Se−Au(III) bonds. The MP2 results show a better agreement with the experimental results, whereas the HF calculations lead to relatively long distances. The distance Au(I)-Au(I) in both models (2.94 and 2.92 Å) is close to that of the original complex at MP2 level (see Table 3). On the other hand, the distance Au^I−Au^{III} in the model with R = −CH$_3$ (3.60 Å (MP2)) is closer to the experimental average (3.64 Å). However, this distance in the system with R = −H is below the experimental value. This implies that the use of the −H ligands bonded to gold(III) produces an exaggeration of the attraction among both metallic centers.

It is also possible to recognize this effect in some angles. For example, the Au(I)-Se−Au(I) angle in both models at MP2 level is close to the experimental value 73°. Whereas the Au(I)-Se−Au(III) angle with R = −CH$_3$ shows the value of 92° at MP2 level, close to the 89° experimental value. However, the angle with R = −H is 80°, which again indicates an exaggerated interaction between Au(I) and Au(III) (see Table 3).

[Se(AuPH$_3$)(AuR$_3$)$_2$]$^-$. We have proposed to study this model, which has no experimental prototype, to estimate the Au^{III}−Au^{III} contact. The clusters (R = −H, −CH$_3$) were optimized following the same lines as described above. In both models the Au^I−Au^{III} distances

Table 5. NBO Charges for the Models

system	method	Au(I)	Au(III)	Se	P	H(bond to Au)	C
[Se(AuPH$_3$)$_2$(AuH$_3$)] (a)	HF	0.39	0.69	−0.94	0.19	−0.15	
	MP2	0.23	0.49	−0.63	0.17	−0.11	
[Se(AuPH$_3$)$_2${Au(CH$_3$)$_3$}] (b)	HF	0.39	0.96	−0.91	0.20		−0.82
	MP2	0.28	0.87	−0.66	0.18		−0.84
[Se(AuPH$_3$)(AuH$_3$)$_2$]$^-$ (c)	HF	0.40	0.71	−0.94	0.21	−0.21	
	MP2	0.23	0.50	−0.68	0.18	−0.18	
[Se(AuPH$_3$){Au(CH$_3$)$_3$}$_2$]- (d)	HF	0.40	0.88	−0.86	0.21		−0.82
	MP2	0.29	0.78	−0.55	0.19		−0.85
[{Se(AuPH$_3$}$_2${Au(CH$_3$)$_2$}$_2$] (e)	HF	0.37	0.89	−0.97	0.20		−0.83
	MP2	0.22	0.67	−0.63	0.17		−0.85

are much shorter than the Au^{III}−Au^{III}, at HF and MP2 levels (see Table 3). However, the [Se(AuPH$_3$)(AuH$_3$)$_2$]$^-$ system shows an overestimated attraction Au−Au at MP2 level, 3.34 and 3.49 Å for Au^I−Au^{III} and Au^{III}−Au^{III}, respectively. In the [Se(AuPH$_3$)(Au(CH$_3$)$_3$)$_2$]$^-$ model, on the other hand, the Au^I−Au^{III} distance is 3.62 Å, and Au^{III}−Au^{III} is 3.97 Å at the MP2 level. The Au^I−Au^{III} distances in the [Se(AuPH$_3$)$_2$(Au(CH$_3$)$_3$)] model are comparable to the observed values.

[Se$_2$(AuPH$_3$)$_2$(Au(CH$_3$)$_2$)$_2$]. This model describes the experimental complex [Se$_2$(AuPPh$_3$)$_2$(Au(C$_6$F$_5$)$_2$)$_2$]. We have optimized the structure assuming C_s symmetry. The results are shown in Tables 3 and 4. Compared with experimental values, the HF Au−Au distances and the Au−Se−Au angles are too large. The results change at the MP2 level; the calculated Au−Au distances are close to the experimental values. A similar trend is observed for the Au−Se−Au angles. Due to the effect of the electronic correlation at the MP2 level, the distances and angles are shorter than at the HF level.

The MP2 calculations are able to reproduce the structural trends found in the experimental complexes. Before proceeding, we wish to compare the charges obtained on the natural bond orbital (NBO)[9] population at the HF and MP2 levels, which are shown in Table 5. The data show in all the models a reduction of the formal oxidation state by the gold and selenium atoms when the calculation methods go from HF to MP2, although the charge distribution on the gold(I) atoms at HF and MP2 levels in the different models does not change substantially. However, the charge on the gold-(III) atoms at the MP2 level is less when the ligand bonded at gold (III) is −H rather than the group −CH$_3$. The −H ligand produces an increase in the charge density on the gold(III), and thus this ligand is not a good model.

Experimental Section

Instrumentation. Infrared spectra were recorded in the range 4000−200 cm^{-1} on a Perkin-Elmer 883 spectrophotometer using Nujol mulls between polyethylene sheets. Conductivities were measured in ca. 5 × 10^{-4} mol dm^{-3} solutions with a Philips 9509 conductimeter. C, H, and S analyses were carried out with a Perkin-Elmer 2400 microanalyzer. Mass spectra were recorded on a VG Autospec, with the LSIMS technique, using nitrobenzyl alcohol as matrix. NMR spectra were recorded on a Varian Unity 300 spectrometer or Bruker ARX 300 spectrometer in CDCl$_3$ (otherwise stated). Chemical shifts are cited relative to SiMe$_4$ (^{1}H, external) and 85% H$_3$-PO$_4$ (^{31}P, external).

Materials. The starting materials [Se(AuPPh$_3$)$_2$],[10] [Se{Au$_2$-(μ-dppf)}],[5] [Au(C$_6$F$_5$)$_3$(OEt$_2$)],[11] and [Au(C$_6$F$_5$)$_2$Cl]$_2$ [12] were prepared by published procedures.

Synthesis of [Se(AuPPh$_3$)$_2${Au(C$_6$F$_5$)$_3$}] (1). To a solution of [Se(AuPPh$_3$)$_2$] (0.100 g, 0.1 mmol) in 20 mL of dichloromethane was added [Au(C$_6$F$_5$)$_3$(OEt$_2$)] (0.0772 g, 0.1 mmol) and the mixture stirred for 15 min. Concentration of the solution to ca. 5 mL and addition of hexane (10 mL) gave complex **1** as a white solid. Yield: 56%. Λ_M = 15 Ω^{-1} cm^2 mol^{-1}. Anal. Found: C, 38.01; H, 1.45. Calcd for C$_{54}$H$_{30}$Au$_3$F$_{15}$P$_2$Se: C, 38.23; H, 1.76. ^{31}P{^{1}H} NMR (δ): room temperature, 35.4 (s); −55 °C, 33.85 (s), 34.65 (s). ^{19}F NMR (δ): −119.1 (m, 4F, *o*-F), −121.6 (m, 2F, *o*-F), −160.40 (t, 1F, *p*-F, ^3J(FF) = 19 Hz), −160.47 (t, 2F, *p*-F, ^2J(FF) = 20 Hz), −163.1 (m, 2F, *m*-F); −55 °C, −118.6 (m, 2F, *o*-F), −119.6 (m, 2F, *o*-F), −122.6 (m, 1F, *o*-F), −122.7 (m, 1F, *o*-F), −158.4 (t, 1F, *p*-F, ^3J(FF) = 21 Hz), −159.4 (t, 2F, *p*-F, ^3J(FF) = 21 Hz), −161.8 (m, 3F, *m*-F), −162.2 (m, 1F, *m*-F), −162.8 (m, 2F, *m*-F).

Synthesis of [Se(AuPPh$_3$)$_2${Au(C$_6$F$_5$)$_3$}$_2$] (2). To a solution of [Se(AuPPh$_3$)$_2$] (0.100 g, 0.1 mmol) in 20 mL of dichloromethane was added [Au(C$_6$F$_5$)$_3$(OEt$_2$)] (0.1544 g, 0.2 mmol) and the mixture stirred for 15 min. Concentration of the solution to ca. 5 mL and addition of hexane (10 mL) gave complex **2** as a white solid. Yield: 60%. Λ_M = 18 Ω^{-1} cm^2 mol^{-1}. Anal. Found: C, 35.87; H, 1.31. Calcd for C$_{72}$H$_{30}$Au$_4$F$_{30}$P$_2$Se: C, 36.12; H, 1.25. ^{31}P{^{1}H} NMR (δ): 35.6 (s). ^{19}F NMR (δ): −120.2 (m, 8F, *o*-F), −122.3 (m, 4F, *o*-F), −156.6 (t, 4F, *p*-F, ^3J(FF) = 20 Hz), −157.1 (t, 2F, *p*-F, ^3J(FF) = 20 Hz), −161.1 (m, 8F, *m*-F), −161.5 (m, 4F, *m*-F).

Synthesis of [{Se(AuPPh$_3$)}$_2${μ-Au(C$_6$F$_5$)$_2$}$_2$] (3). To a solution of [Se(AuPPh$_3$)$_2$] (0.200 g, 0.2 mmol) in 20 mL of dichloromethane was added [Au(C$_6$F$_5$)$_2$Cl]$_2$ (0.1133 g, 0.1 mmol) and the mixture stirred for 15 min. Concentration of the solution to ca. 5 mL and addition of diethyl ether (10 mL) gave complex **3** as a white solid. Yield: 55%. Λ_M = 9 Ω^{-1} cm^2 mol^{-1}. ^{31}P{^{1}H} NMR (δ): 37.8 (s, 2P, AuPPh$_3$), 33.8 (s, 1P, [AuCl(PPh$_3$)]). ^{19}F NMR (δ): room temperature, −120.9 (m, 8F, *o*-F), −158.3 (t, 4F, *p*-F, ^3J(FF) = 20 Hz), −161.8 (m, 8F, *m*-F); −55 °C, −120.8 (m, 4F, *o*-F), −121.0 (m, 4F, *o*-F), −157.4 (t, 4F, *p*-F, ^3J(FF) = 21 Hz), −160.8 (m, 4F, *m*-F), −161.3 (m, 4F, *m*-F).

Synthesis of [Se{Au$_2$(μ-dppf)}{Au(C$_6$F$_5$)$_3$}] (4). To a solution of [Se{Au$_2$(μ-dppf)}] (0.102 g, 0.1 mmol) in 20 mL of dichloromethane was added [Au(C$_6$F$_5$)$_3$(OEt$_2$)] (0.0772 g, 0.1 mmol) and the mixture stirred for 15 min. Concentration of the solution to ca. 5 mL and addition of hexane (10 mL) gave complex **2** as an orange solid. Yield: 66%. Λ_M 1.4 Ω^{-1} cm^2 mol^{-1}. Anal. Found: C, 36.40; H, 1.75. Calcd for C$_{52}$H$_{28}$Au$_3$F$_{15}$-FeP$_2$Se: C, 36.17; H, 1.62. ^{1}H NMR (δ): room temperature, 4.5 (m, br, 4H, C$_5$H$_4$), 3.9 (m, br, 4H, C$_5$H$_4$); −55 °C, 5.01 (m, 1H, C$_5$H$_4$), 4.92 (m, 1H, C$_5$H$_4$), 4.47 (m, 2H, C$_5$H$_4$), 4.23 (m, 1H, C$_5$H$_4$), 4.02 (m, 1H, C$_5$H$_4$), 3.35 (m, 1H, C$_5$H$_4$), 4.29 (m, 1H, C$_5$H$_4$). Room temperature ^{31}P{^{1}H} NMR (δ): 28.8 (s); −55 °C, 28.9 (s), 27.1 (s). ^{19}F NMR (δ): room temperature, −118.7 (m, 4F, *o*-F), −122.5 (m, 2F, *o*-F), −158.7 (t, 2F, *p*-F, ^3J(FF) = 21.3 Hz), −159.7 (t, 1F, *p*-F, ^3J(FF) = 19.2 Hz), −162.7 (m, 2F,

(9) Raghavachari, K.; Trucks, G. W. *J. Phys. Chem.* **1989**, *91*, 2457.

(10) Jones, P. G.; Thöne, C. *Chem. Ber.* **1991**, *124*, 2725.
(11) Usón, A.; Laguna, A.; Laguna, M.; Jiménez, J.; Durana, E. *Inorg. Chim. Acta* **1990**, *168*, 89.
(12) Usón, A.; Laguna, A.; Laguna, M.; Abad, A. *J. Organomet. Chem.* **1983**, *249*, 437.

Table 6. Basis Sets and Pseudopotentials (PPs) Used in the Present Work

atom	PP	VE	basis	remarks
H			(4s1p)/[2s1p]	$\alpha_p = 0.80$
C	Bergner	4	(4s4p1d)/[2s2p1d]	$\alpha_d = 0.80$
P	Bergner	5	(4s4p1d)/[2s2p1d]	$\alpha_d = 0.34$
Se	Bergner	6	(4s4p1d)/[2s2p1d]	$\alpha_d = 0.25$
Au	Andrae	19	(8s6p5d1f)/[6s5p3d1f]	$\alpha_f = 0.20$

m-F), −162.9 (m, 4F, m-F); −55 °C, −117.1 (m, 2F, o-F), −119.9 (m, 2F, o-F), −122.7 (m, 2F, o-F), −157.7 (t, 2F, p-F, $^3J(FF) = 20.0$ Hz), −158.7 (t, 1F, p-F, $^3J(FF) = 20.9$ Hz), −161.6 (m, 2F, m-F), −161.7 (m, 2F, m-F), −162.3 (m, 2F, m-F).

Synthesis of [Se{Au₂(μ-dppf)}{Au(C₆F₅)₃}₂] (5). To a solution of [Se{Au₂(μ-dppf)}] (0.102 g, 0.1 mmol) in 20 mL of dichloromethane was added [Au(C₆F₅)₃(OEt₂)] (0.1544 g, 0.2 mmol) and the mixture stirred for 15 min. Concentration of the solution to ca. 5 mL and addition of hexane (10 mL) gave complex **5** as an orange solid. Yield: 60%. Λ_M 8.3 Ω^{-1} cm² mol⁻¹. Anal. Found: C, 34.96; H, 1.27. Calcd for $C_{70}H_{28}Au_4F_{30}$-FeP_2Se: C, 34.67; H, 1.15. ¹H NMR (δ): room temperature, 4.35 (m, 4H, C₅H₄), 3.50 (m, 4H, C₅H₄); −55 ° C, 4.56 (m, 2H, C₅H₄), 4.40 (m, 2H, C₅H₄), 4.16 (m, 2H, C₅H₄), 3.31 (m, 2H, C₅H₄). ³¹P{¹H} NMR (δ): room temperature, 29.5 (s); −55 °C, 28.7 (s, 2P, $^2J(PSe) = 484$ Hz). ¹⁹F NMR (δ): room temperature, −121.7 (m, 4F, o-F), −122.3 (m, 8F, o-F), −156.3 (t, 4F, p-F, $^3J(FF) = 20$ Hz), −157.1 (t, 2F, p-F, $^3J(FF) = 20$ Hz), −161.4 (m, 12F, m-F); −55 °C, −119.5 (m, 4F, o-F), −122.4 (m, 4F, o-F), −122.5 (m, 4F, o-F), −155.9 (t, 4F, p-F, $^3J(FF) = 20$ Hz), −156.5 (t, 2F, p-F, $^3J(FF) = 20$ Hz), −160.5 (m, 4F, m-F), −160.8 (m, 4F, m-F), −161.6 (m, 4F, m-F).

Crystal Structure Determinations. The crystals were mounted in inert oil on glass fibers and transferred to the cold gas stream of the Siemens P4 diffractometer. Data were collected using monochromated Mo Kα radiation ($\lambda = 0.71073$ Å) in ω-scan mode (**3**) or θ–2θ (**4**). Absorption corrections were applied on the basis of Ψ-scans. The structures were solved by the heavy-atom method and refined on F^2 using the program SHELXL-97.¹³ All non-hydrogen atoms were refined anisotropically except for solvent. Hydrogen atoms were included using a riding model. Further crystal data are given in Table 6. *Special details of refinement:* The dichloromethane solvent in **3** is disordered over an inversion center. In **4** the dichloromethane is disordered over two positions, and further solvent regions were tentatively identified as a pentane and an ethanol molecule. These assignments, and the associated occupation factors and derived parameters, should obviously be interpreted with caution.

Gaussian 98 Calculations. The Gaussian 98 package¹⁴ was used. The basis sets and pseudopotentials (PP) used in the production runs are given in Table 7. The 19-valence-electron (VE) quasi-relativistic (QR) pseudopotential (PP) of Andrae¹⁵ was employed for gold. We have employed one f-type polarization function for Au. The f orbital is necessary for the weak intermolecular interactions, as was demonstrated previously for various metals.⁴ The atoms C, P, and Se were also

Table 7. Details of Data Collection and Structure Refinement for Complexes 3 and 4

	3	**4**
chem formula	$C_{61}H_{32}Au_4Cl_2$-$F_{20}P_2Se_2$	$C_{60}H_{48}Au_3Cl_2F_{15}$-$FeOP_2Se$
cryst habit	colorless plate	orange tablet
cryst size/mm	$0.40 \times 0.25 \times 0.10$	$0.70 \times 0.30 \times 0.10$
cryst syst	triclinic	triclinic
space group	$P\bar{1}$	$P\bar{1}$
a/Å	9.4464(12)	12.344(2)
b/Å	12.4953(14)	17.362(2)
c/Å	14.279(2)	17.889(3)
α/deg	102.892(10)	97.78(10)
β/deg	92.724(10)	108.15(10)
γ/deg	99.303(10)	109.65(10)
U/Å³	1515.2(4)	3305.2(9)
Z	1	2
D_c/g cm⁻³	2.286	1.38
M	2223.49	1928.53
$F(000)$	1026	1824
T/°C	−100	−100
$2\theta_{max}$/deg	50	50
μ(Mo Kα)/mm⁻¹	10.41	7.61
transmissn	0.409, 0.990	0.5165, 0.0758
no. of rflns measd	6025	12 286
no. of unique rflns	5652	11 290
R_{int}	0.0262	0.051
$R(F > 4\sigma(F))^a$	0.0318	0.0477
$R_w(F^2$, all rflns)^b	0.0613	0.1332
no. of rflns used	5652	11 290
no. of params	409	744
no. of restraints	365	698
S^c	0.878	1.038
max $\Delta\rho$/e Å⁻³	1.196	1.61

^{a} $R(F) = \sum ||F_o| - |F_c|/\sum|F_o|$. ^{b} $R_w(F^2) = [\sum\{w(F_o^2 - F_c^2)^2\}/\sum\{w(F_o^2)^2\}]^{0.5}$; $w^{-1} = s^2(F_o^2) + (aP)^2 + bP$, where $P = [F_o^2 + 2F_c^2]/3$ and a and b are constants adjusted by the program. ^{c} $S = [\sum\{w(F_o^2 - F_c^2)^2\}/(n - p)]^{0.5}$, where n is the number of data and p the number of parameters.

treated by Stuttgart pseudopotentials,¹⁶ including only the valence electron for each atom. For these atoms, double-ζ basis sets were used, augmented by d-type polarization functions. For the H atom, a double-ζ plus one p-type polarization function was used (see Table 6).¹⁷

We have optimized the structures for the models [Se-(AuPH₃)₂(AuR₃)] (R = −H, −CH₃; C_s), [Se(AuPH₃)(AuR₃)₂]⁻ (R = −H, −CH₃; C_s), and [Se₂(AuPH₃)₂(Au(CH₃)₂)₂] (C_s) at the Hartree−Fock (HF) and second-order Møller−Plesset perturbation theory (MP2) levels (see Figure 3). In the experimental structures, the triphenylphosphine, −P(C₆H₅)₃, is replaced by −PH₃, the ferrocene-bridged ligands by −H, and −C₆F₅ by −H and −CH₃. The original ligands would involve a large computational effort. If the rotation of the terminal −PH₃ and −CH₃ ligands would have broken the symmetry, their dihedral angle was fixed.

Supporting Information Available: Two X-ray crystallographic files, in CIF format, for complexes **3** and **4**. This material is available free of charge via the Internet http://pubs.acs.org.

OM010474M

(13) Sheldrick, G. M. SHELXL-97, a Program for Crystal Structure Refinement; University of Göttingen, Göttingen, Germany, 1997.

(14) Frisch, M. J.; Trucks, G. W.; Schlegel, H. B.; Scuseria, G. E.; Robb, M. A.; Cheeseman, J. R.; Zakrzewski, V. G.; Montgomery, J. A., Jr.; Stratmann, R. E.; Burant, J. C.; Dapprich, S.; Millam, J. M.; Daniels, A. D.; Kudin, K. N.; Strain, M. C.; Farkas, O.; Tomasi, J.; Barone, V.; Cossi, M.; Cammi, R.; Mennucci, B.; Pomelli, C.; Adamo, C.; Clifford, S.; Ochterski, J.; Petersson, G. A.; Ayala, P. Y.; Cui, Q.; Morokuma, K.; Malick, D. K.; Rabuck, A. D.; Raghavachari, K.; Foresman, J. B.; Cioslowski, J.; Ortiz, J. V.; Stefanov, B. B.; Liu, G.; Liashenko, A.; Piskorz, P.; Komaromi, I.; Gomperts, R.; Martin, R. L.; Fox, D. J.; Keith, T.; Al-Laham, M. A.; Peng, C. Y.; Nanayakkara, A.; Gonzalez, C.; Challacombe, M.; Gill, P. M. W.; Johnson, B. G.; Chen, W.; Wong, M. W.; Andres, J. L.; Head-Gordon, M.; Replogle, E. S.; Pople, J. A. *Gaussian 98*; Gaussian, Inc.: Pittsburgh, PA, 1998.

(15) Andrae, D.; Häusserman, M.; Dolg, H.; Stool, H.; Preuss, H. *Theor. Chim. Acta* **1990**, *77*, 123.

(16) Bergner, A.; Dolg, M.; Küchle, W.; Stoll, H.; Preuss, H. *Mol. Phys.* **1993**, *80*, 1431.

(17) Dunning, T. H.; Hay, P. J. In *Modern Theoretical Chemistry*; Schaefer, H. F., III, Ed.; Plenum Press: New York, 1997; Vol. 3, pp 1−28.